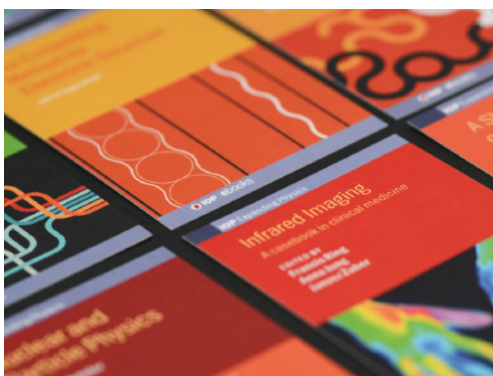


PAPER

An affordable method to produce CuInS_2 'mechano-targets' for film deposition

To cite this article: D Delmonte *et al* 2020 *Semicond. Sci. Technol.* **35** 045026

View the [article online](#) for updates and enhancements.




IOP | ebooks™

Bringing together innovative digital publishing with leading authors from the global scientific community.

Start exploring the collection—download the first chapter of every title for free.

An affordable method to produce CuInS_2 ‘mechano-targets’ for film deposition

D Delmonte¹ , R Manfredi¹, D Calestani¹, F Mezzadri^{1,2}, L Righi^{1,2}, M Mazzer¹, F Pattini¹, S Rampino¹, G Spaggiari³ and E Gilioli¹

¹CNR-IMEM, Parco Area delle Scienze 37A, I-43124 Parma, Italy

²Dipartimento SCVSA, Università degli Studi di Parma, Parco Area delle Scienze 17A, I-43124 Parma, Italy

³Dipartimento Scienze Fisiche Matematiche ed Informatiche, Università degli Studi di Parma, Parco Area delle Scienze 7A, I-43124 Parma, Italy

E-mail: davide.delmonte@imem.cnr.it

Received 20 December 2019, revised 17 January 2020

Accepted for publication 13 February 2020

Published 19 March 2020



CrossMark

Abstract

We report on the room temperature, simple and cheap preparation by mechano-synthesis of polycrystalline targets of complex sulphide semiconductors, namely CuInS_2 (CIS), to be used for film deposition in physical vacuum techniques such as PLD, sputtering or LT-PED. The sulphur (S)-based targets usually require expensive high pressure equipment to compensate the high S vapour pressure; nevertheless they are indispensable for the deposition of high band-gap semiconductor materials. The comparison of CIS films grown by mechano-synthesis and by commercial targets demonstrates similar material quality, making the mechano-synthesis a viable solution in the fabrication of high band-gap, S-based targets of complex chalcogenides.

Supplementary material for this article is available [online](#)

Keywords: mechanochemistry, high-energy ball milling, photovoltaic semiconductors, chalcogenides, pulsed electron deposition, thin film solar cells

(Some figures may appear in colour only in the online journal)

1. Introduction

One of the main issues of the physical vacuum deposition (PVD) techniques is the availability of good quality targets that largely determine the quality of the coating.

The most common target preparation (solid state reaction or ceramic method), involves the following steps: stoichiometric weighing of the starting reagents, grinding and mixing, calcination, cold uniaxial pressing and sintering. In order to increase the strength of the pellets, a volatile binding agent, removed during the sintering process, is often used. The process is rapid, simple and cheap. The main disadvantage is the need of high processing temperatures; the densification of the target material, i.e. the reduction of porosity, is determined by the sintering temperature and duration. A serious complication arises whenever one or more elements possess a high vapour pressure, implying the use of high pressure synthesis to compensate the tendency of the volatile element(s) to evaporate.

This is the typical case of complex chalcogenides, in particular sulphides; among various applications, they are widely used as absorbers for the fabrication of thin film solar cells, owing to their high light absorption coefficient as for the chalcogenide Cu(In,Ga)(Se,S)_2 (or CIS) and kesterite $\text{Cu}_2\text{ZnSn(S,Se)}_4$ (or CZTS) compounds.

The physical and chemical techniques commonly used for the deposition of CIS and CZTS films are basically based on complex multi-step processes, starting from the elements or binary (selenides, sulphides) compounds, i.e. DC magnetron sputtering, reactive sputtering, or thermal evaporation of the metal alloy followed by selenization/sulphurization, co-evaporation of elements (Cu, In and S), molecular beam epitaxy, spray pyrolysis, chemical vapour deposition, atomic layer deposition, solvothermal method, electrochemical deposition, etc ([1] and references therein).

In the search for simple and low cost methods, the deposition of the absorber in a single-stage process by means

of PVD techniques operating on ternary/quaternary targets is extremely appealing, aiming to transfer the complex stoichiometry of the CIS/CZTS from the bulky target to the growing film. This would allow the growth of films with complex CIS/CZTS stoichiometry by using bulk target, without the need of successive expensive and environmentally impacting treatments such as selenization (involving toxic H_2Se). Single-stage deposition from a stoichiometric ternary/quaternary target has been reported for CIG(Se,S)- and CZT(Se,S)-based thin film solar cells by RF-Sputtering [2], Pulsed Laser Deposition (PLD) [3], and Low Temperature Pulsed Electron Deposition (LT-PED) [4]. In particular, the latter technique allows the deposition of stoichiometric and high quality CIGS films without needing any selenization treatments at high temperature, exploiting the high internal energy of adatoms generated by the pulsed electron beam ablation to form ordered and flat CIGS layers even at low growth temperature ($<300^\circ C$) [5]. This peculiar feature of LT-PED allowed the single stage deposition of conventional [6] and bifacial [7] CIGSe-based thin film solar cells with photovoltaic conversion efficiency of 17%.

One of the main properties of these compounds is represented by the tuning of the band gap value through the balance of Se/S ratio; for example, it can be varied from 1.04 (CISe) to 1.53 eV (CIS) [8] or from 0.95 (CZTSe) to 1.50 eV (CZTS) [9]. The search for high band gap materials for solar cells is challenging, in particular in the emerging field of the tandem cells on Silicon, suited to achieve photovoltaic conversion efficiency exceeding 30% [10]; therefore the availability of targets of sulphides or with high S/Se ratio represents an issue to address.

The sulphur-based targets are generally synthesized under high pressure to compensate the high S vapour pressure (P_s), preventing its evaporation. The simpler equation for S vapour pressure [11] is:

$$\ln P_s(\text{Pa}) = 204.74 - 18166/T(\text{K}) - 27.433 \ln(T) + 0.017432T \quad (1)$$

resulting in a P_s value of about 200 atm. at $1050^\circ C$.

For comparison, the simplified equation for Se vapour pressure [12], P_{Se} , is:

$$\text{Log}_{10} P_{Se}(\text{atm}) = -5043/T(\text{K}) + 5.265, \quad (2)$$

leading to a value of P_{Se} of about 26 atm. at $1050^\circ C$.

Due to this huge difference between P_{Se} and P_s , commercial multi-element targets of complex selenides can be easily found, but very few companies provide the sulphides counterparts. They usually do not disclose the fabrication method in details, however CIS targets can be synthesized by HIP (hot isostatic pressing) at $T \geq 700^\circ C$ and $P > 220$ atm starting from $Cu_2S + In_2S_3$ powders for reaction time ≥ 1 h [13].

Besides the cost of the commercial targets, to better control the material quality and composition, some groups synthesize their own multi-elements targets. At CNR-IMEM, the CISe/CIGSe targets are synthesized at $1050^\circ C$ in a modified Czochralski reactor, previously converted for the synthesis from molten elements of high purity targets of III-V

and II-VI semiconductors [14]. This process allows to accurately preserve the stoichiometry of the starting elements (5N purity grade Cu, In, Ga and Se), for the combination of the physical encapsulation (by molten B_2O_3 and/or semi-closed crucibles) and the high inert gas counter pressure (Argon, $30 \div 40$ bar), preventing the Se evaporation. The obtained high quality Se-based targets allowed the LT-PED fabrication of the above-mentioned 17%-efficient solar cells. On the other hand, due to the higher P_s , the corresponding sulphide (CIS/CIGS) targets cannot be prepared with this method; according to the equation (1), P_s is about 200 bar at $1050^\circ C$, exceeding by far the process limit.

A novel, easy and affordable alternative to produce CIS dense targets suitable for PVD, is represented by mechanochemical (MC) reaction of CIS powders starting from binary sulphides (Cu_2S and In_2S_3) in a high-energy planetary ball milling process followed by low temperature sintering.

Besides the conventional use as powder grinding, ball milling techniques are also effective tools to perform solid state reactions. Mechanochemistry by milling process [15, 16] has been applied in different synthesis areas, as supramolecular chemistry [17], metal-organic complexes [18], organic molecules [19] or inorganic oxides [20] but rarely to the synthesis of complex sulphides, such as kesterites (CZTS and CZTSe) for solar cell applications [21, 22].

The mechanism responsible for the reaction activation is the mechanical energy exchanged through the elastic impact of the balls against the precursor powders during the milling. One of the most plausible model, the Magma plasma model [23, 24] estimates a sudden energy increase which determines a local temperature enhancement up to 10 000 K. Such an amount of energy transfer induces the formation of dislocations responsible for the desegregation of the grains, leading to strongly defected and chemical activated surfaces. The huge statistical number of impacts determines a rapid increase of the grains' surface to volume ratio favouring the chemical reaction of the precursors; therefore, MC can be seen as a surface-guided solid state synthesis. In this work we first study the MC reaction process to obtain large amounts (few grams per synthesis) of single phase CIS. Then, we define a simple two-step sintering treatment of the MC powders to obtain a target suitable for film deposition by vacuum deposition techniques. The target (hereafter 'mechano-target') is successfully used to deposit CIS film by LT-PED; the comparison with a commercial CIS target prepared by Hot Isostatic Press (HIP), demonstrates that MC is a viable option to obtain targets of complex sulphides.

2. Methods

The CIS powders are obtained starting from the binary sulphides (Cu_2S 99.5% Alfa Aesar, In_2S_3 99.99% Aldrich) by mechano-chemical reaction without any liquid solvent and in air atmosphere, using a Pulverisette 7 (Fritsch) planetary ball milling, equipped with agate pots (volume: 45 ml) and a variable number of agate balls (diameter: 10 mm). The conditions for the CIS formation are determined by the

combination of three independent parameters: (1) rotational speed (RPM, from 10 to 800 rounds per minute), (2) the ball-to-powder mass ratio (BPR) and (3) reaction time (TIME).

The powder composition and the thin films crystallographic orientation are studied by x-ray diffraction (XRD), using a Siemens D500 system with a Cu $K\alpha$ x-ray source ($\lambda = 1.54 \text{ \AA}$) in Bragg–Brentano geometry, while the morphology and the composition is investigated by Scanning Electron Microscopy (SEM, Philips 515) working at 25 kV and equipped with energy dispersive x-ray spectrometry apparatus (EDS, EDAX Phoenix with Si:Li detector). A 3 mm thick target is sintered through a two-step process: 5/6 g of MC powders are pressed into a 1 inch cylindrical mold at 25 tons per 1.5 h in a manual hydraulic press and annealed in oven for 18 h at 135 °C in ambient atmosphere. The mechano-target composition is checked after the thermal treatment.

The CIS films are deposited by the low temperature pulsed electron deposition (LT-PED, PEBS-21, Neocera) on an unheated glass substrate at 16 kV, in a pure Ar atmosphere (3×10^{-3} mbar) using a CIS mechano-target glued on a rotating metallic target holder, following the process reported in previous works [6, 25]. It is worth noting that these conditions have been optimized for ‘conventional’ or commercial Se-containing targets and no specific adjustment has been adopted for the S-based mechano-targets.

In situ plasma plume composition is monitored by optical emission spectrometry (OES), (Hamamatsu Mini Spectrometer, Series TM) in the 200–800 nm range. Raman spectroscopy (using a Horiba Jobin–Yvon Labram micro-Raman apparatus) is used for phase analysis of the CIS films. Reflectance spectra of CIS thin films are collected using a Jasco V-770 Spectrophotometer in the 500 ÷ 1600 nm range.

3. Results and discussion

3.1. MC-CIS powder synthesis and characterization

The CIS formation and the evolution of the chemical reaction: $\text{Cu}_2\text{S} + \text{In}_2\text{S}_3 \rightarrow 2\text{CuInS}_2$ is studied as a function of RPM, BPR and TIME in dry conditions. The details of the optimization of the CIS phase and purity can be found in tables S1–S2 reported as supplementary information available online at stacks.iop.org/SST/35/045026/mmedia. The CIS powders can be obtained in pure form in the RPM range: 300–700, BPR: 30–125 fixing TIME = 1 h, following the experimental stability law: $\text{RPM} = K_{\text{CIS}}/\text{min}(\text{BPR})$, where $K_{\text{CIS}} = (27700 \pm 3500)$ rpm, extrapolated from the MC phase diagram of CIS (see table S1 reported as supplementary information available at [link]).

To the best of our knowledge, the only work on the formation of CIS by MC reaction is reported by E Dutkova *et al* at RPM: 550 rpm and TIME: 30–120 min starting from the elements in tungsten carbide milling chamber [26]. By comparison with the corresponding selenides, T Wada *et al* found RPM: 250 rpm and TIME: 60 min as best conditions for the mechano-synthesis of CISe from elemental $\text{Cu} + \text{In} + 2\text{Se}$ [27] and A E Zaghi *et al* RPM: 350 rpm and

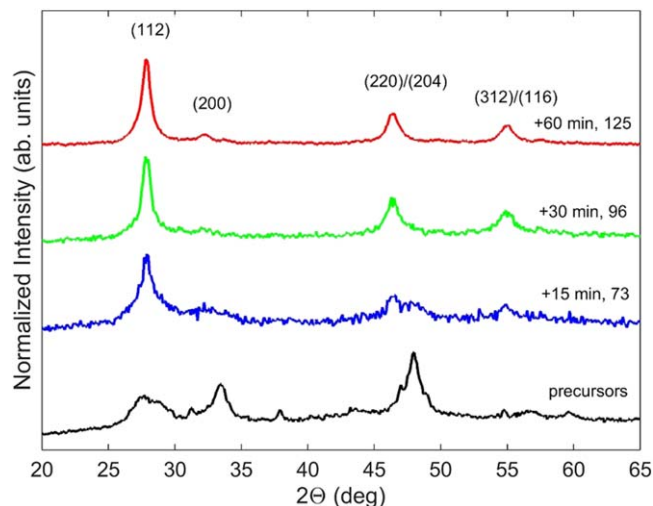


Figure 1. CIS phase formation versus time studied by PXRD from precursors (a). RPM = 500 and initial BPR = 73.

TIME: 120 min followed by wet milling at RPM: 350 rpm and TIME: 120–300 min to get nanometric powders of Cu–In–Se alloy from pure elements [28].

The chemical reaction induced by the MS process is rapid; the time evolution (figure 1) shows the CIS chalcopyrite as the main phase already after 15' and in pure form at 30'. The width of the diffraction peaks indicate the low crystallinity of the obtained powders. Noteworthy, during the reaction (between the first minutes to 30' of milling time) the strong deterioration of the precursors crystallinity as well as the simultaneous emergence of the CIS phase peaks (blue pattern in figure 1) are observed, suggesting that the reaction starts when the precursors' crystallites surface become dominant with respect to the volume.

In order to increase the amount of CIS powders produced by a single synthesis, suitable for the target production, it is important to minimize the BPR to increase the quantity of precursors in the same pot, standing the number of balls. According to the CIS MC phase diagram (table S1 reported as supplementary information available online at stacks.iop.org/SST/35/045026/mmedia) and verified the right composition of the product (table S2 reported as supplementary information available at [link]), the best synthesis parameters are RPM = 700, BPR = 30 and for TIME = 1h. Under these conditions, the PXRD shows the presence of CIS without spurious phases (figure 2(a)). The PXRD analysis confirms the expected tetragonal cell (Space Group $I-42d$), with $a = b = 5.524 \text{ \AA}$, $c = 11.141 \text{ \AA}$ and cell volume = 339.84 \AA^3 .

Applying the Sherrer formula on the diffraction peaks, the average single crystallite's dimension was estimated around 9 nm. The SEM images (figure 2(b)) show a narrow grain distribution and highlight also a diffused coalescence (microsinterization mechanism) of the powders at the microscale; specifically, the majority of particles are sub-micrometric (500 ÷ 700 nm), while few supermicrometric CIS clusters are laid on the microsintered layer (i.e. white large particles in figure 2(b)). SEM-EDS analysis shows the stoichiometric distribution of the CIS atomic composition, i.e.

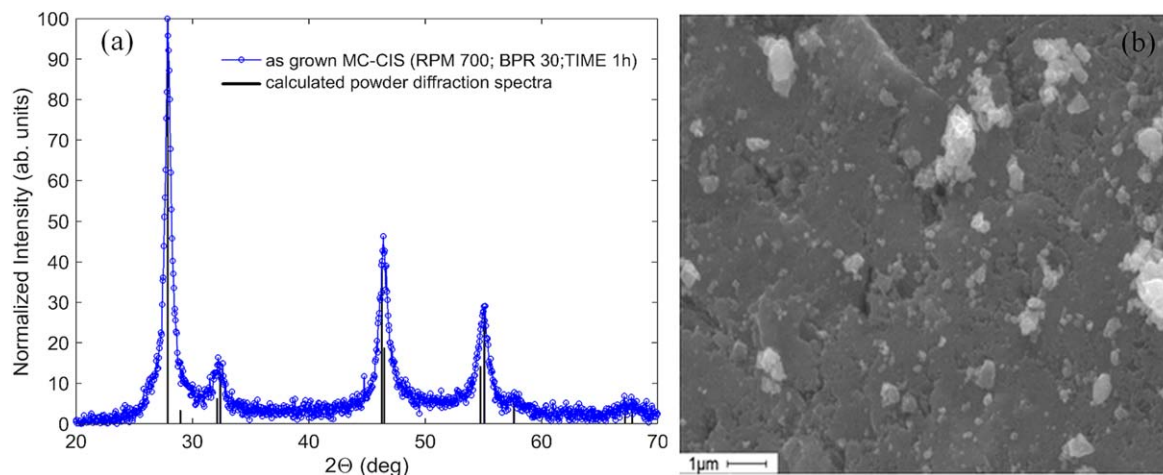


Figure 2. PXRD pattern of a CIS sample grown at RPM = 700 and BPR = 30 for TIME = 1 h (a) and corresponding SEM planar view (b).

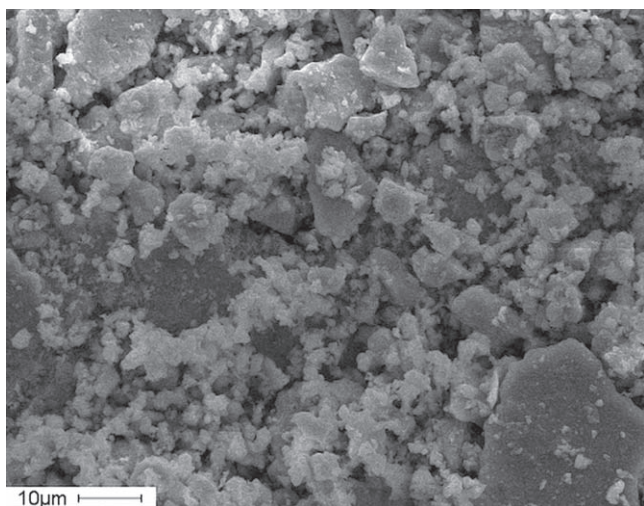


Figure 3. SEM image collected after a CIS MC reaction at RPM = 700, BPR = 30 and TIME = 4 h.

Cu 24.9%, In 24.2% and S 50.9% (see table 1), indicating that the MC reaction does not cause any sulphur loss. Moreover, eventual agate losses formed by the erosion of pots and balls during the milling process, if present, are below the threshold of sensitivity of both PXRD and EDS detection.

For longer milling time at the same RPM and BPR, the coalescence experienced in figure 2(b) is destroyed by the continuous exchange of the mechanical energy so that the formation of larger clusters become favoured; at the same time the inhomogeneity increases abruptly, as displayed in figure 3. Possibly, the smaller particles are likely kinetically driven to aggregate in larger clusters in a process that leads to the aggregation of the smaller grains.

3.2. Target sintering

For the target preparation, 6 g of CIS as grown after MC synthesis carried out with RPM = 700 BPR = 30 and TIME = 1 h, are sintered by applying 25 tons/inch² (cold pressing) for 1.5 h and then annealed for 18 h at 135 °C in a

Table 1. SEM-EDS atomic composition of the MC-CIS powders, MC and HIP targets and corresponding films grown by LT-PED.

Sample	Cu (%)	In (%)	S (%)
As-grown MC powders	24.9	24.2	50.9
Sintered MC target	24.7	24.3	51.0
LT-PED film from MC target	23.2	27.3	49.5
Commercial HIP Target	25.1	25.0	49.9
LT-PED film from HIP target	23.1	27.2	49.7

conventional oven in ambient atmosphere (see figure S1 reported as supplementary information available online at stacks.iop.org/SST/35/045026/mmedia).

PXRD pattern confirms the absence of spurious phases and highlights negligible variations of the peak width (figure 4); the compositional analysis, performed by SEM-EDS on the target, shows that there are no sulphur losses up to 180 °C and that the powder stoichiometry is fully retained (table 1).

The obtained MC-target looks dense and compact by SEM analysis (figure 5); its density, by the geometrical calculation of the disc is (3.95 ± 0.35) g/cm³, lower than the CIS ideal density of 4.73 g/cm³.

3.3. Film deposition by LT-PED

The deposition of CIS thin films by LT-PED using the CIS mechano-target and a commercial target sintered by HIP, performed under the same conditions, is compared. Although the LT-PED working conditions strongly depend on the target quality and density (the density of the HIP target is 4.59 g/cm³, 97% the theoretical density and significantly higher than the mechano target), the ‘*in situ*’ analysis of the LT-PED plume composition by OES spectroscopy reveals that the ablation efficiency using HIP and MS CIS targets is essentially the same, generating a plasma plume with similar compositions (see figure S2 reported as supplementary information available online at stacks.iop.org/SST/35/045026/mmedia).

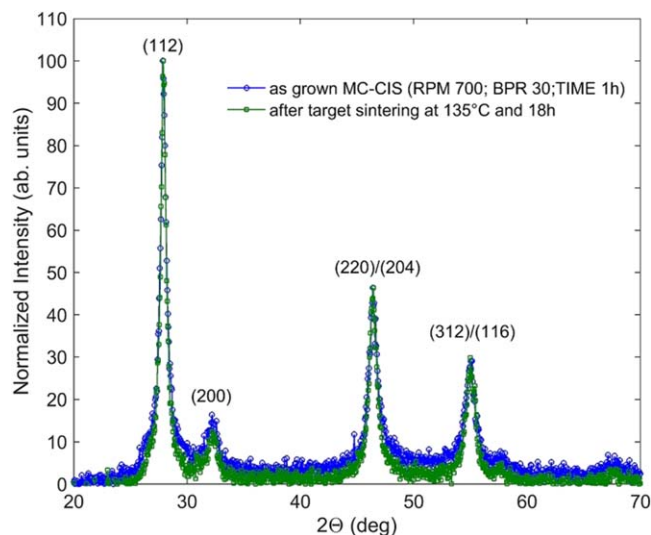


Figure 4. PXRD of as-grown MC-CIS powders (blue line) and mechano-target (red line).

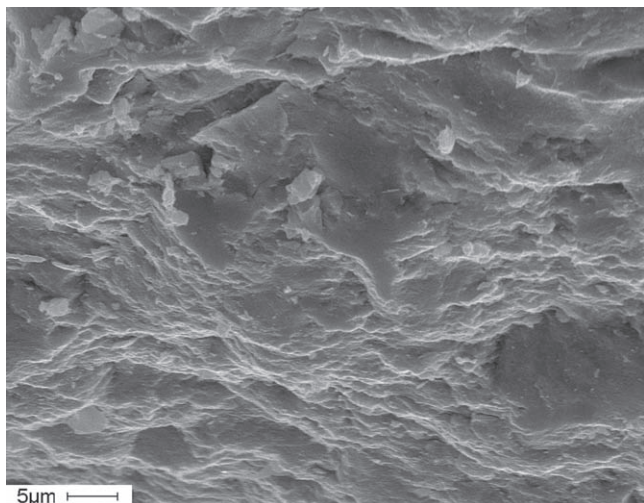


Figure 5. Cross-section SEM view of the CIS sintered target.

The deposited film grown from the MC target looks uniform and homogeneous on $1 \times 1''$ substrate, with a good superficial adhesion (it endures the standard ‘scotch test’, see figure S3(a) reported as supplementary information available online at stacks.iop.org/SST/35/045026/mmedia). The deposition rate is about 0.1 nm/pulse, which is in the same range measured for CIGSe.²² The corresponding XRD pattern on 1.7 μm thick film (figure 6) shows that the phase is strongly oriented along the (112) direction, fully comparable with the CIS film from the HIP target in terms of phase, purity and orientation (see the HIP film picture in figure S3(b) reported as supplementary information available online at stacks.iop.org/SST/35/045026/mmedia).

The Raman spectra collected for the MC and HIP targets are similar, as shown in figures 7(a)–(b). Interestingly, the spectra of the corresponding films are even more similar exhibiting the same peaks, the first around 298 cm^{-1} as a result of mode A1-CH (290 cm^{-1}) and mode A1-CA (305 cm^{-1})

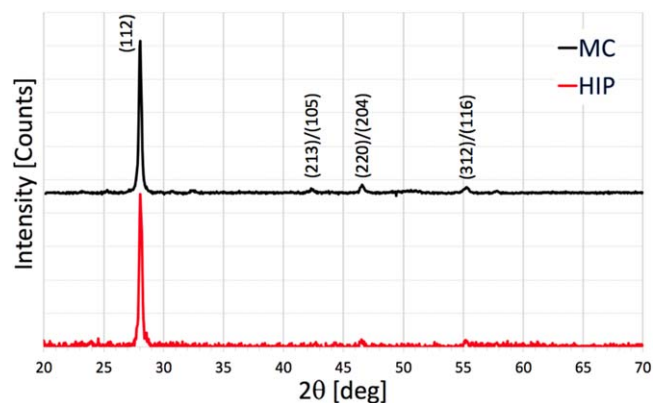


Figure 6. (a) XRD patterns of the films grown by LT-PED starting from MC and HIP targets (black and red patterns, respectively).

convolution and the second in the $340\text{--}350 \text{ cm}^{-1}$ range (mode B2 and E^1 convolution), proving again the same films quality (see figure 6) [29].

The optical bandgap of CIS films is calculated by transforming the reflectance spectra as proposed by Kumar [30]: a similar bandgap value of 1.45–1.46 eV is found for both films grown from the HIP and MC targets, respectively (see figure S4 reported as supplementary information available online at stacks.iop.org/SST/35/045026/mmedia).

The compositional analysis performed by SEM-EDS on the target confirms that there are no sulphur losses up to 180°C and the stoichiometric ratio is retained after the sinterization (table 1).

Table 1 clearly confirms the efficient material transfer from the mechano-target to the growing film, that is one of the main characteristics of the LT-PED technique. The slight Cu-deficiency observed in thin films is due to the unavoidable presence of evaporation beside the ablation mechanisms on the target, as verified in previous works [6, 31].

The SEM images in planar and cross-section, reported in figures 8(a)–(b), display the typical morphology of a chalcopyrite films deposited by LT-PED. The presence of some microsized droplets on the surface is a common feature of the high-energy deposition techniques [32, 33]. However, no signs of larger target debris were observed on the surface, indicating that the hardness of the sintered mechano-target is sufficient to prevent the ejection of big chunks toward the growing CIS film. Although the optimization of CIS-based thin film solar cells from the mechano-target goes beyond the scope of the present paper, this would be clearly an important opportunity. In this perspective, these chunks may act as shunting paths when CIS is used as absorber layer in a solar cell, thus reducing the overall device performance.

4. Conclusion

The deposition of complex sulphides films by PVD can be efficiently and reproducibly performed by using a sintered target obtained by mechano-synthesis (MC) from the binary sulphides. This method is by far simpler and cheaper than

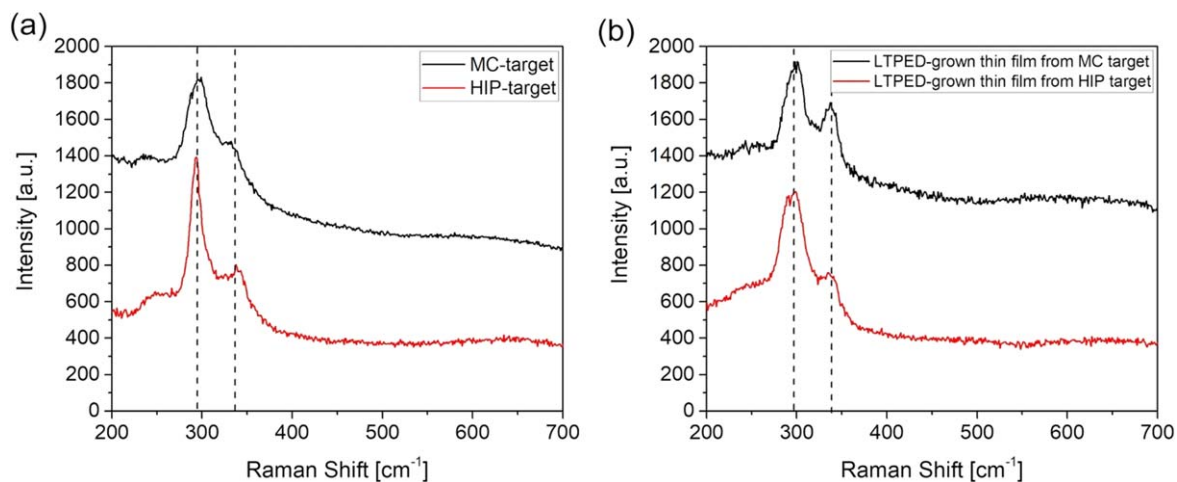


Figure 7. Raman spectra of bulk MC and HIP CIS target (a) and corresponding film by LT-PED (b). Dashed lines highlight the value of the A1-CH and A1-CA convolution peak and the value of B2 and E¹ convolution peak.

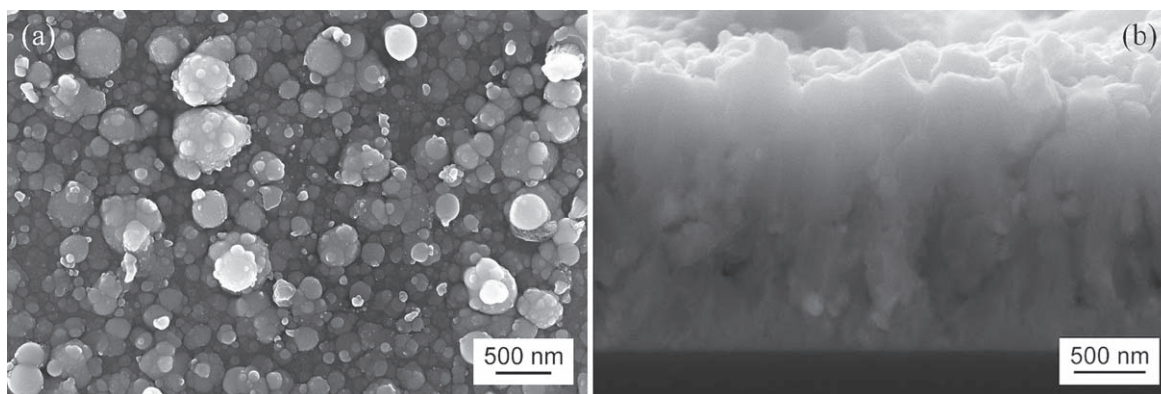


Figure 8. SEM planar image of the surface (a) and cross-section of CIS film deposited by LT-PED from a mechano-target (b).

using targets from high pressure (HIP) treatment, necessary whenever high vapour pressure elements (like S) are present.

To test this, we report the deposition of CIS thin films by LT-PED using a mechano-target, sintered at low temperature from MC pure powders, as potential high bandgap absorber in the photovoltaic field.

By comparing its structural (XRD), morphological (SEM) and compositional (EDS and Raman) properties with films grown under the same conditions from a commercial target sintered by HIP, we demonstrate that the properties of the two materials are essentially the same, providing a simple method to prepare high quality targets for complex sulphides film deposition.

Acknowledgments

The authors acknowledge M Bronzoni, A Sala (CNR-IMEM), D Bersani (University of Parma) for fruitful discussion, P Ferro (CNR-IMEM) for XRD and L Fornari and E Del Canale (CNR-IMEM and University of Parma) for the MC optimization process.

ORCID iDs

D Delmonte  <https://orcid.org/0000-0001-5367-527X>

References

- [1] Ramanujam J and Singh U P 2017 *Energy Environ. Sci.* **10** 1306–19
- [2] Park J C, Al-Jassim M, Lee B-T and Kim T W 2020 *J. Alloys Compd.* **212** 152065
- [3] Chen C C, Qi X, Chang W C, Tsai M G, Chen I G, Lin C Y, Wu P H and Chang K P 2015 *Appl. Surf. Sci.* **351** 772–8
- [4] Bronzoni M, Stefancich M and Rampino S 2012 *Thin Solid Films* **520** 7054–61
- [5] Rampino S, Gilioli E, Bissoli F and Pattini F 2013 *Prog. Photovolt.: Res. Appl.* **21** 588–94
- [6] Mazzer M *et al* 2016 *Energies* **9** 207
- [7] Mazzer M *et al* 2017 *Sol. Energ. Mater. Sol. C* **166** 247–53
- [8] Haight R, Barkhouse A, Gunawan O, Shin B, Copel M, Hopstaken M and Mitzi D B 2011 *Appl. Phys. Lett.* **98** 253502
- [9] Stanbery B J 2002 Copper indium selenides and related materials for photovoltaic devices *Crit. Rev. Solid State Mater. Sci.* **27** 73–117
- [10] White T P, Lal N N and Catchpole K R 2014 *IEEE J. Photovolt.* **4** 208–14

- [11] Peng D Y and Zhao J 2011 *J. Chem. Thermodyn.* **33** 1121–31
- [12] Baker E H 1968 *J. Chem. Soc. A* 1089–92
- [13] Kodigala S R 2011 *Cu(In_{1-x}Gax)Se₂ Based Thin Film Solar Cells* (Cambridge Massachusetts: Academic Press)
- [14] Zappettini A, Zha M, Marchini L and Calestani D 2012 *CrystEngComm* **14** 5992–5
- [15] Baláž P 2008 *Mechanochemistry in Nanoscience and Minerals Engineering* (Berlin: Springer)
- [16] James S L et al 2012 *Chem. Soc. Rev.* **41** 413
- [17] Friščić T 2012 *Chem. Soc. Rev.* **41** 3493–510
- [18] Lazuen-Garay A, Pichon A and James S L 2007 *Chem. Soc. Rev.* **36** 846–55
- [19] Shearouse W C, Korte C M and Mack J 2011 *Green Chem.* **13** 598–601
- [20] Šepelák V, Bégin-Colin S and Le Caër G 2012 *Dalton Trans.* **41** 11927–48
- [21] Shyju T S, Anandhi S, Suriakarthick R, Gopalakrishnan R and Kuppusami P 2015 *J. Solid State Chem.* **227** 165–77
- [22] Pulgarín-Agudelo F A, Vigil-Galán O, Nicolás-Marín M M, Courel M, González R, Mendoza-Leon H, Velumani S, Rohini M, Andrade-Arvizu J A and Oliva F 2017 *Mater. Res. Express* **4** 12
- [23] Thiessen P A, Meyer K and Heinicke G 1967 *Grundlagen der Tribochemie* (Berlin: Akademie Verlag)
- [24] Thiessen K P 1979 *Z. Phys. Chem.* **260** 403–440.
- [25] Rampino S et al 2012 *Appl. Phys. Lett.* **101** 132107
- [26] Dutkova E, Sayague M J, Briancin J, Zorkovska A, Bujnakova Z, Kováč J, Kováč J Jr, Balaz P and Ficeriová J 2016 *J. Mater. Sci.* **51** 1978–84
- [27] Wada T, Kinoshita H and Kawata H S 2003 *Thin Solid Films* **431–432** 11–5
- [28] Zaghi A E, Buffière M, Brammertz G, Batuk M, Lenaers N, Kniknie B, Hadermann J, Meuris M, Poortmans J and Vleugels J 2014 *Adv. Powder Technol.* **25** 1254–61
- [29] Moreau A, Insignares-Cuello C, Escoubas L, Simon J J, Bermúdez V, Pérez-Rodríguez A, Izquierdo-Roca V and Ruiz C M 2015 *Sol. Energy Mater. Sol. Cells* **139** 101–7
- [30] Kumar V, Sharma S K, Sharma T P and Singh V 1999 *Opt. Mater.* **12** 115–9
- [31] Pattini F, Bronzoni M, Mezzadri F, Bissoli F, Gilioli E and Rampino S 2013 *J. Phys. D: Appl. Phys.* **46** 245101
- [32] Fähler S, Störmer M and Krebs H U 1997 *Appl. Surf. Sci.* **109–110** 433–6
- [33] Rampino S, Pattini F, Malagù C, Pozzetti L, Stefancich M and Bronzoni M 2014 *Thin Solid Films* **562** 307–13